# Gümüşhane University Journal of Science

# Adsorption of methylene blue dye onto alginate-bioglass membranes: response surface method, isotherm, and kinetic studies

*Metilen mavisi boyasının aljinat-biyocam membranlara adsorpsiyonu: Cevap yüzey yöntemi, izoterm ve kinetik çalışmalar*

## Hasan TÜRE *[1] 🆔

*[1] Ordu Üniversitesi, Fatsa Deniz Bilimleri Fakültesi, Deniz Bilimleri ve Teknolojisi Mühendisliği Bölümü, 52200, Ordu*

**Abstract**

In this research, environment-friendly composite membranes based on alginate (ALG) and bioglass nanoparticles (BGs) were prepared by the solvent casting technique and utilized as adsorbents for the elimination of methylene blue (MB) from water. Zeta potential of the particles was determined to be -24.9 mV by laser dynamic light scattering (DLS), and their sizes were found to be 773 and 777 nm by transmission electron microscopy (TEM) and DLS analysis, respectively. Atomic force microscope (AFM) analysis revealed that increasing the BGs content from 1 to 5% w/v caused the root mean square roughness of membranes to increase from 159.38 to 182.03 nm. The adsorption process was successfully modeled and optimized using a hybrid response surface methodology integrated central composite design (RSM-CCD). A statistical analysis was utilized to examine and optimize the effects of three important independent variables (concentration of BGs (1-5% w/v), pH of the solution (3-9), and initial dye level (15-45 mg L$^{-1}$)) on MB adsorption performance. The findings indicated that the quadratic model was suitable for prediction of MB's removal. Optimized experimental parameters were found to be a pH of 9, a contact time of 120 min, an initial MB concentration of 45 mg L$^{-1}$, and a BGs concentration of 1% (w/v). Freundlich isotherm and pseudo-second-order kinetic models were found to be the best-fitting models in isotherm and kinetic studies, respectively. Dubinin-Radushkevich (D-R) isotherm model predicted a chemical mechanism for MB adsorption onto the composite alginate membranes.

**Keywords:** Alginate, Bioactive glass, Methylene blue, Optimization, Response surface method

*Öz*

*Bu çalışmada, solvent çözücü döküm yöntemi ile aljinat (ALG) ve biyocam nanopartikül (BGs) bazlı çevre dostu kompozit membranlar hazırlanmış ve metilen mavisinin (MB) sudan uzaklaştırılması için adsorban olarak kullanılmıştır. Partiküllerin zeta potansiyeli, lazer dinamik ışık saçılımı (DLS) ile -24,9 mV olarak belirlenmiş ve boyutları, transmisyon elektron mikroskobu (TEM) ve DLS analizi ile sırasıyla 773 ve 777 nm olarak bulunmuştur. Atomik kuvvet mikroskobu (AFM) analizi, BGs içeriğinin %1'den %5'e çıkarılmasının, membranların karekök ortalama pürüzlülüğünün 159,38 nm'den 182,03 nm'ye çıkmasına neden olduğunu ortaya koymuştur. Adsorpsiyon süreci, hibrit cevap yüzey metodolojisi ile bütünleşmiş merkezi bileşik tasarım (RSM-CCD) kullanılarak başarılı bir şekilde modellenmiş ve optimize edilmiştir. Üç önemli bağımsız değişkenin (BGs konsantrasyonu (%1-5 a/h), solüsyonun pH'ı (3- 9), ve başlangıç boya konsantrasyonu (15-45 mg L$^{-1}$)) MB adsorpsiyon kapasitesi üzerindeki etkilerini değerlendirmek ve optimize etmek için istatistiksel analiz gerçekleştirilmiştir. Sonuçlar, ikinci dereceden modelin MB'nin uzaklaştırılmasının tahmini için uygun olduğunu ortaya koymuştur. Optimize edilmiş deneysel parametreler, pH=9, 120 dk temas süresi, 45 mg L$^{-1}$ başlangıç MB konsantrasyonu ve %1 (a/h) BGs konsantrasyonu olarak tespit edilmiştir. Freundlich izotermi ve yalancı ikinci dereceden kinetik modellerinin sırasıyla izoterm ve kinetik çalışmalarda en uygun modeller olduğu bulunmuştur. Dubinin-Radushkevich (D-R) izoterm modeli, kompozit aljinat membranlara MB adsorpsiyonu için kimyasal bir mekanizma öngörmüştür.*

*Anahtar kelimeler: Aljinat, Biyoaktif cam, Metilen mavisi, Optimizasyon, Cevap yüzey yöntemi*

* Hasan TÜRE; hasanture@odu.edu.tr

# 1. Introduction

Hazardous dye concentrations in waste water are increasing as a result of industrial activity, which has been considered a significant environmental issue worldwide (Oladipo et al., 2014; Tkaczyk et al., 2020). Many treatment approaches, such as chemical coagulation, various forms of oxidation processes, and biological processes, are being investigated for elimination of toxic dyes like methylene blue (MB) (Nidheesh et al., 2018; Katheresan et al., 2018; Baloch et al., 2018). Adsorption is regarded as promising treatment approach among these because of its affordability, simplicity, eco-friendliness, and high efficacy (Dlamini et al., 2020). Elimination of dyes from aqueous solutions has been accomplished over the last few decades using a variety of natural and synthetic adsorbents (Zhou et al., 2019; Mensah et al., 2022; Suba & Rathika, 2016). However, due to technological or economic limitations, the majority of these adsorbents were not applied on a widespread scale. Thus, there is a significant need for the creation of new, inexpensive adsorbents that are also effective, such as those made of natural materials (Allouss et al., 2019).

A silica-based material, such as bioglass (BGs), has a wide range of uses as catalytic support, adsorbents, and catalysts owing to its superior surface qualities when compared to zeolites and clays. Because of the surfaces' negative charges, BGs can be considered good MB adsorbents (Li et al., 2016). However, the use of BGs in powder form restricts their recovery and reusability (Godiya et al., 2019). Designing composite adsorbents by incorporating BGs into biopolymers could be considered one of the most efficient approaches to address this problem.

Due to their affordability, biocompatibility, and environmental friendliness, natural polysaccharide-based adsorbents like sodium alginate (ALG) have recently attracted a lot of attention for their ability to eliminate water contaminants. (Godiya et al., 2019; Sabbagh et al., 2021; Wang et al., 2019). Furthermore, existence of hydroxyl and carboxylic groups on ALG makes it a promising adsorbent for electrostatic interactions with cationic dyes (Djelad et al., 2019). ALG has been demonstrated to form promising composite adsorbents with organic and inorganic components, and both composites were shown to be efficient at MB adsorption (Alver et al., 2020; Boukoussa et al., 2021; Boukhalfa et al., 2019). Numerous operating factors interact nonlinearly during the adsorption process. Owing to the high number of experimental runs and time commitment, the comman and traditional strategy for adsorption optimization seems to be no longer practical in this situation (Allouss et al., 2019; Karimifard & Moghaddam, 2018). The adsorption process is optimized by researchers utilizing statistical experimental design methods like response surface methodology (RSM) to overcome these limits. RSM is known as an effective mathematical and statistical method for carrying out experiments and building models by simultaneously changing a number of operating factors. RSM's main objective is to establish ideal working conditions quickly and with the fewest possible experiments (Ma et al., 2019). Among the several response surfaces designs, the central composite design (CCD) is one of the most effective and fruitful designs because it can evaluate variables of the quadratic model, produce serial designs, and notice a model-related lack of fit (Sabbagh et al., 2021). As far as I'm aware, no research has been done on removal of MB from aqueous solutions utilizing ALG-BGs membranes with precision RSM-CCD-based optimization.

In this study, BGs were prepared using the Stöber method, and then alginate membranes including varying concentrations of BGs (1, 3, and 5% w/v) were produced using the solvent casting approach, which was then crosslinked with calcium chloride. The developed membranes were used as adsorbents to take MB out of water.

Variables affecting MB removal efficiency, such as initial MB level, BGs level, and solution pH, were optimized using RSM-CCD. Furthermore, the obtained data were analyzed using isotherms (Langmuir, Freundlich, and Dubinin-Radushkevich) and kinetics (pseudo-first-order and pseudo-second-order) models to better examine adsorption behavior and mechanism. It should be noted that characterization of obtained samples is not the primary aim of this study.

## 2. Material and method

### 2.1. Materials

Ethanol (98%), calcium nitrate tetrahydrate (99%), sodium alginate, and tetraethyl orthosilicate (TEOS, 98%) were purchased from Sigma-Aldrich, Germany. Ammonium hydroxide (28%), HCl, $CaCl_2$, and NaOH were received from Tekkim, Turkey. MB was provided from Pancreac, Spain.

### 2.2. Synthesis of bioglass

The BGs were synthesized according to my previous work (Türe, 2019). Briefly, a solution including 10 ml of ethanol, 4.5 ml of ammonium hydroxide, and 15 ml of deionized water was incorporated into another solution having 25 ml of ethanol and 3 ml of TEOS. After 30 minutes of stirring, 1.59 g of calcium nitrate tetrahydrate were added. The suspension was mixed for 90 minutes and centrifuged at 5000 rpm for 10 minutes. Resulting slurry was then rinsed with a water-and-ethanol solution (2:10 v/v). Then, leftovers were dried overnight at 60 °C and calcined for 2 hours at 700 °C.

### 2.3. Preparation of bioglass-containing alginate membranes

ALG powder was dissolved in deionized water utilizing magnetic stirrer at 25°C to obtain an ALG mixture (2% w/v). To make BGs-filled alginate membranes, a suitable number of BGs (1, 3, and 5% w/v) was added to solution, which was then homogenized at 2000 rpm for 20 minutes (WVR VDI 25, Germany). Then, the obtained solution was sonicated using a digital ultrasonic bath (WF-UD6, 50 kHz, Turkey) for 30 minutes at 40 °C. After that, mixture was put into petri dishes and dried for 48 hours at 40 °C. Following the drying stage, the films were removed from the petri plates and were cut into 25-mm-diameter discs. Then, the prepared films were soaked in 100 mL of a 2% (w/v) $CaCl_2$ solution for 10 minutes to allow cross-linking. Finally, films were treated several times with deionized water to eliminate any remaining $CaCl_2$ and dried for 24 hours at 40 °C. Samples are coded based on the amount of bioglass they contain; for example, ALG-1 is a membrane that includes 1% (w/v) BGs.

### 2.4. Transmission electron microscopy (TEM)

BGs were dissolved in deionized water using magnetic stirrer for 10 minutes at a concentration of roughly 0.1 g/L for TEM examination. Thereafter, a transmission electron microscope was used to quickly collect micrographs after pipetting a single drop of solution onto a carbon-coated grid without any additional steps. (Hitachi HighTech HT7700, Japan).

### 2.5. Analysis of the zeta potential, particle size, and the polydispersity index of BGs

A laser-based dynamic light scattering device (Malvern Instruments, UK) was utilized to measure the zeta potential, polydispersity index (PDI), and particle size of BGs at room temperature. Measurements were carried out after suspending the powdered BGs in water at pH 6.4.

### 2.6. Atomic force microscopy (AFM)

Tapping mode was used to perform AFM measurements (Picoforce SPM, US). Standard silicon cantilevers with spring constants of 40 N $m^{-1}$ were utilized. Maximum scan rate used for the measurements was 1 Hz. Three AFM height pictures taken at three separate locations on the membranes were used to calculate the root mean square roughness (Rq).

### 2.7. Process variables and RSM

BGs concentration, pH of the MB solution, and initial MB level were chosen as three independent variables to examine their effects. These factors were selected in accordance with publications in the literature on dye adsorption and the results of preliminary laboratory tests. Contact time, agitation speed, and temperature were set at 120 minutes, 150 rpm, and 25±2 °C, respectively. Design-Expert statistical software package 8.0 was utilized to create all of the trials, producing 20 runs for the face central CCD mode (Table 1).

**Table 1.** CCD experimentation factors and levels

| Factors | | | Levels |
| --- | --- | --- | --- |
| (A) pH | Low | Central | High |
| (B) BGs concentration (w/v) | | | |
| (C) Initial dye concentration (mg/L) | (-1) | 0 | (+1) |
| Runs | A | B | C |
| 1 | 3 | 1 | 15 |
| 2 | 3 | 5 | 15 |
| 3 | 3 | 3 | 30 |
| 4 | 3 | 1 | 45 |
| 5 | 3 | 5 | 45 |
| 6 | 6 | 3 | 15 |
| 7 | 6 | 1 | 30 |
| 8 | 6 | 3 | 30 |
| 9 | 6 | 3 | 30 |
| 10 | 6 | 3 | 30 |
| 11 | 6 | 3 | 30 |
| 12 | 6 | 3 | 30 |
| 13 | 6 | 3 | 30 |
| 14 | 6 | 5 | 30 |
| 15 | 6 | 3 | 45 |
| 16 | 9 | 1 | 15 |
| 17 | 9 | 5 | 15 |
| 18 | 9 | 3 | 30 |
| 19 | 9 | 1 | 45 |
| 20 | 9 | 5 | 45 |

## 2.8. Adsorption experiments

Adsorption studies were carried out in beakers including 25 mL of a known concentration of MB solution (15-45 mg/L) and an adequate weight of ALG-BGs membranes. The beakers were shaken in an orbital shaker (WiseCube, WIS-20R, Germany) at a constant speed of 150 rpm for 120 minutes. Adsorption experiments were performed at 25 ±2 °C and at pH (3- 9). Based on the RSM-CCD approach, operating parameters including BGs concentration, initial MB level, and pH were researched and adjusted for maximal MB elimination. Following the reaction period, the membranes were simply removed, and amount of the dye adsorption was evaluated utilizing a UV-vis spectrophotometer (Shimadzu-UVmini-1240) at 664 nm. The following formula was used to get the adsorption capacity:

$$Q_e = \frac{(C_o - C_e) \, x \, V}{m} \qquad (1)$$

where $C_e$ (mg/L) and $C_0$ (mg/L) are equilibrium and initial dye levels, respectively; $m$ (g) is weight of dry adsorbent, and $V$ (L) is volume of dye solution.

## 3. Results and discussion

### 3.1. Characterization of adsorbents

The particles were spherical in form and had an average diameter of 773 nm, according to TEM analysis (Figure 1). The size of the obtained particles was estimated by DLS analysis to be 777 nm, which is in line with the result of TEM analysis. The particles displayed a narrow particle size distribution with a PDI of about 0.3, which is typical of highly monodispersed systems, according to DLS analysis (Mostafa et al., 2021). DLS analysis also showed that the particles' zeta potential was found to be -24.9 mV, indicating that the BGs were negatively charged and thus sufficiently stable in water to be used in the development of composite membranes

(Zheng et al., 2017; Zheng et al., 2018). In the previous study, it was detected that zeta potential value and the size of the particles obtained by same method were higher. The reason for this can be clarified by the fact that the addition of copper causes an increase in the diameter and zeta potential value of the particles (Türe, 2019).
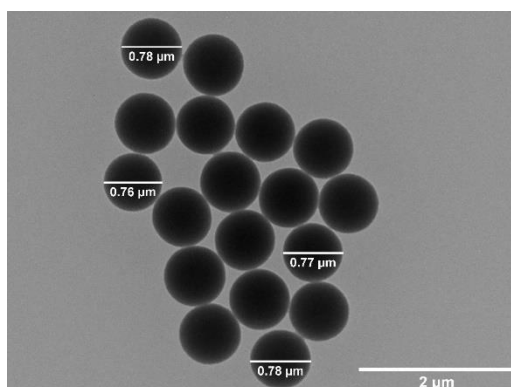


**Figure 1.** TEM image of obtained BGs particles

The AFM 3D-surface images of the ALG-1, ALG-3, and ALG-5 samples are demonstrated in Figure 2
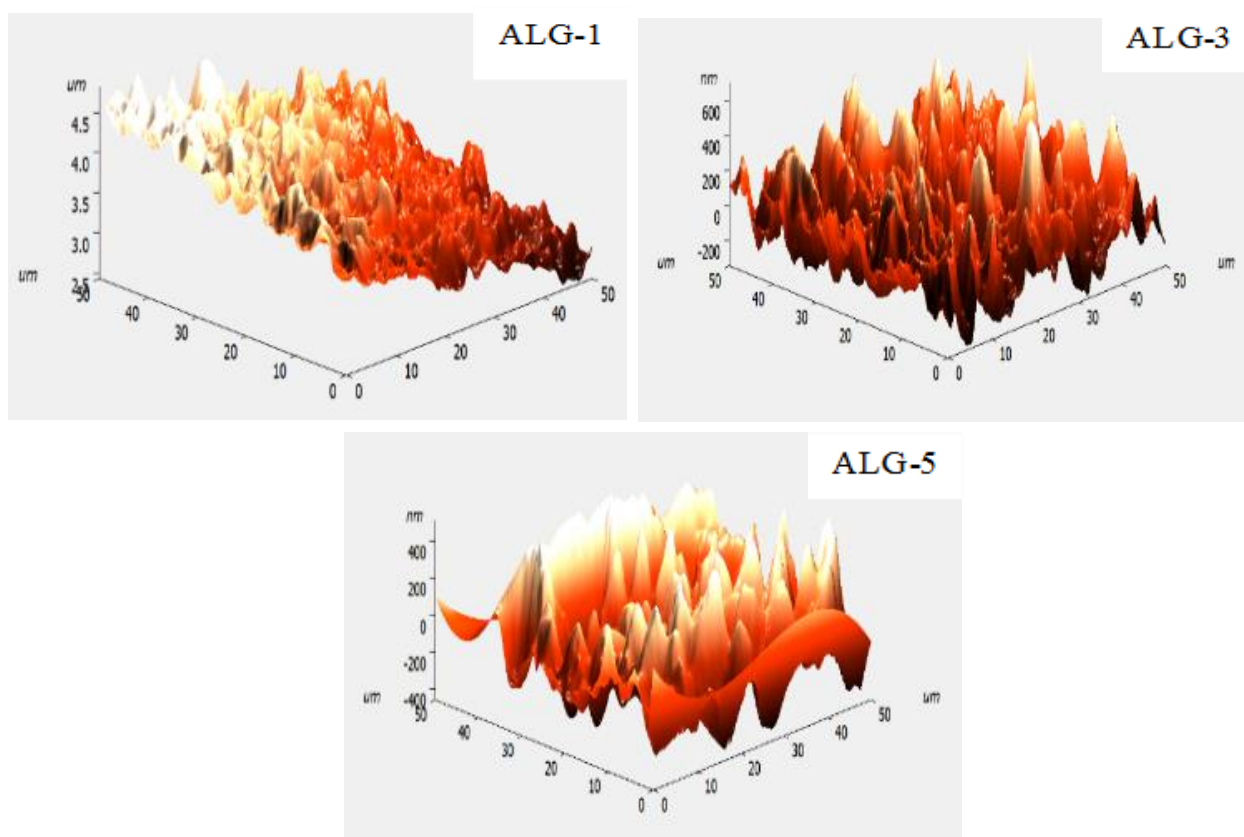


**Figure 2.** AFM-3D surface ALG membranes containing 1-5 % w/v BGs

AFM was used to assess the roughness of alginate membranes and the effect of BGs addition. The Rq values of ALG-1, ALG-3 and ALG-5 membranes were calculated as 159.38, 168.17 and 182.03, respectively. More uniform BGs dispersion and homogenous morphological structures produced by intermolecular interactions between various phase constituents are two factors that contribute to lower surface roughness (Abdullah et al., 2019). Dziadek et al. (2015) also reported surface roughness increased when bioactive glass particles were incorporated into Poly($\varepsilon$-caprolactone) films. The properties of bioglass-containing alginate membranes, such as swelling, mechanical properties, and interactions between ALG and BGs, can be obtained from my previously published work (Türe, 2019).

## 3.2. RSM modeling using CCD

The typical "one factor at a time" optimization used in adsorption procedures to achieve maximal dye removal is time-consuming and labor-intensive. RSM has recently been shown to be a successful strategy for reducing experimentation costs and time. In this section of the experiment, RSM and CCD were used to determine the ideal circumstances for removing MB from ALG-BGs membranes (Al-Sakkari et al., 2020). The following second-order polynomial equation represents the most prevalent empirical model in RSM that explains how design parameters relate to response (Allouss et al., 2019).

$$Y = \beta_0 + \sum_{i=1}^{k} \beta_i x_i + \sum_{i=1}^{k}\sum_{j=i+1}^{k} \beta_{ij} x_i x_j + \sum_{i=1}^{k} \beta_{ii} x_i^2 \tag{2}$$

where, $\beta_0$ represents constant coefficient, coefficients for linear, interaction, and quadratic terms are $\beta_i$, $\beta_{ij}$ and $\beta_{ii}$ li, respectively, $k$ indicates number of independent factors, $x_i$ and $x_j$ are input variables, and $Y$ is predicted response used as dependent variable.

The mathematical equation that explains how the current adsorption process responds to three selected variables given by the software is as follows:

$$Q_e = 15.08 + 0.13A - 1.25B + 4.74C + 0.02AB + 0.54AC - 0.46BC - 0.30A^2 + 0.35B^2 - 1.01C^2 \tag{3}$$

**Table 2.** ANOVA analysis of MB removal

| Source | Sum of squares | d$f$ | $F$-value | $p$ value | |
|---|---|---|---|---|---|
| **Model** | 249.39 | 9 | 120.63 | <0.0001 | significant |
| **A** | 0.1701 | 1 | 0.7406 | 0.4096 | |
| **B** | 15.66 | 1 | 68.19 | <0.0001 | |
| **C** | 224.38 | 1 | 976.76 | <0.0001 | |
| **AB** | 0.0042 | 1 | 0.0182 | 0.8952 | |
| **AC** | 2.31 | 1 | 10.06 | 0.01 | |
| **BC** | 1.71 | 1 | 7.43 | 0.0213 | |
| **A$^2$** | 0.2418 | 1 | 1.05 | 0.3291 | |
| **B$^2$** | 0.3415 | 1 | 1.49 | 0.2507 | |
| **C$^2$** | 2.79 | 1 | 12.12 | 0.0059 | |
| **Residual** | 2.30 | 10 | | | |
| **Lack-of-fit** | 0.9887 | 5 | 0.7556 | 0.6170 | not significant |
| **Pure error** | 1.31 | 5 | | | |
| **Cor total** | 251.69 | 19 | | | |
| **R$^2$** | 0.9909 | | | | |
| **R$^2$ Adj** | 0.9827 | | | | |

The information in Table 2 shows the $R^2$ value (0.9909) and adjusted $R^2$ value (0.9827 values) are highly correlated and, as a result, are in good settlement for quadratic model. This implies a link between process variables and response, which is very well explained by quadratic model. The $R^2$ value of 0.9909 shows that proposed mathematical model can explain 99.09% of the total variation in MB adsorption data and that it cannot explain just 0.91% of the total variation. According to the ANOVA findings (Table 2), model's $F$-level of 120.63 and $p$-level of 0.0001 indicate it is statistically important. Furthermore, $p$-values were used to assess the relevance of each of linear terms (A, B, and C), interaction terms (AB, AC, and BC), and quadratic terms (A$^2$, B2, and C$^2$) on the response. The literature states that a $p$-value of less than 0.05 for each factor in an ANOVA table indicates that related factor is significant at a 95% confidence level. Since the $p$-values for the BGs concentration (B), initial dye concentration (C), AC, BC, and C$^2$ are all less than 5%, these terms were all chosen as highly important model terms. Terms B (BGs concentration) and C (initial dye level) in the tested range are important parameters favorably affecting the MB adsorption on ALG-BGs, based on data in Table 2. Term B has negative coefficient values, indicating that these factors have a negative impact on response (i.e., adsorption capacity declines). According to the results of the ANOVA, lack of fit is not important in comparison to error, so that model adequately explains the data (Marzban et al., 2021).

In Figure 3, 3D-response surface plots for the MB adsorption capacity illustrate graphical representations of the regression equation. From these graphical representations, it is obvious that capacity of MB adsorbed gets increased with a rise in the initial MB level, which enhances interaction between MB and ALG-BGs membranes. pH of solution had little impact on adsorption process, and increasing the pH was beneficial. Marzban et al. (2021) reported a similar observation in alginate beads containing kaolin. However, the adsorption capability of the membranes reduced as the BGs concentration increased. Optimized experimental parameters providing the highest measured MB removal (99.56%) are: agitation speed of 150 rpm, T = 25±2 ∘C, initial dye concentration of 45 mg$^{-1}$, time of 120 min, pH of 9, 0.05 g, and BGs concentration of 1% (w/v).
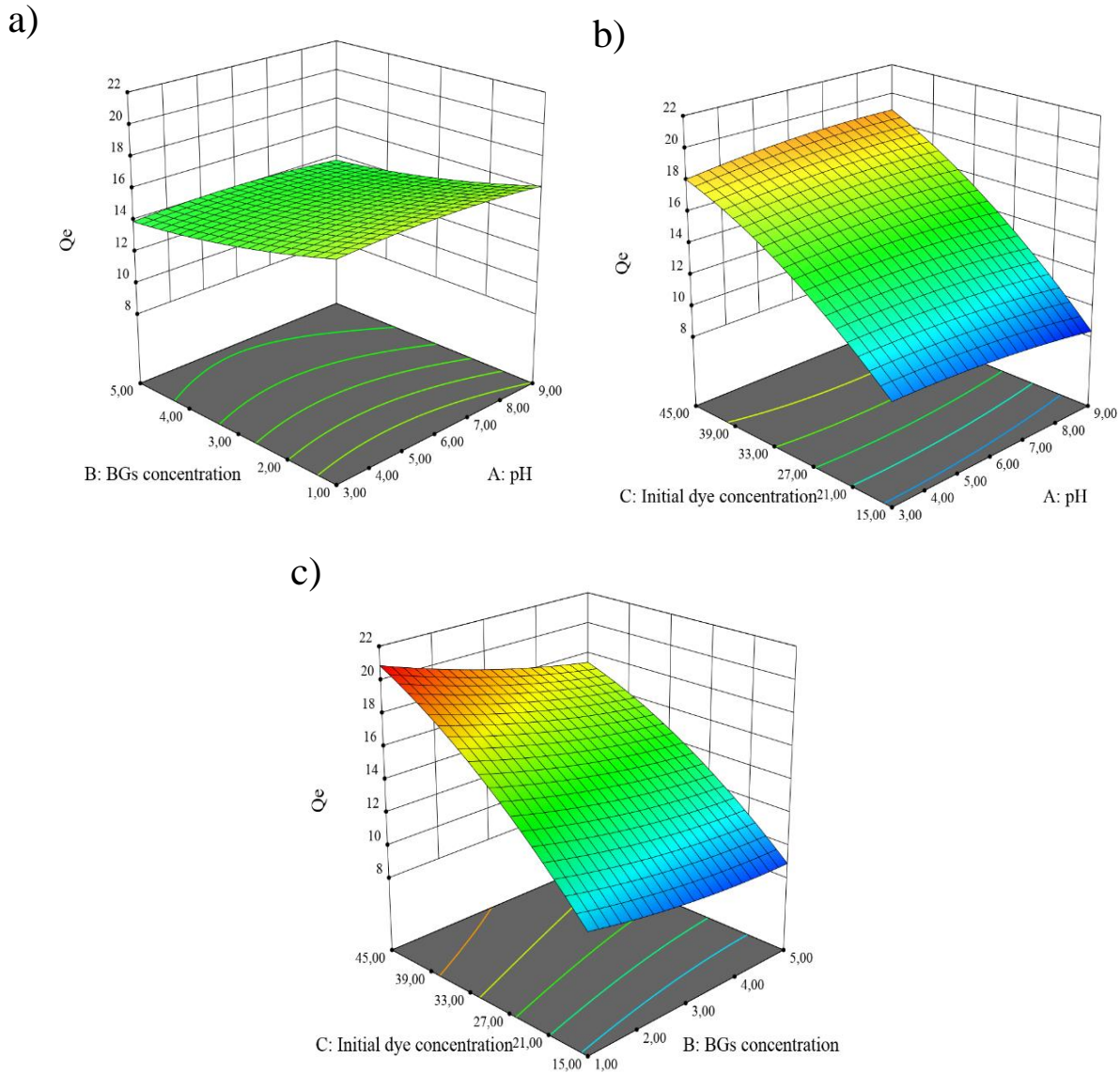
**Figure 3.** Effects of (a) BGs concentration-pH, (b) initial dye level-pH, and (c) initial dye concentration-BGs level on yield of MB elimination by ALG-1 membranes are shown in 3D surface plots

## 3.3. Verification of models

To validate the model, comparison graphs and diagnostic plots have been studied. The residuals' placement close to the straight line, as seen in Figure 4, supports the model's fitting. Figure 5(a) shows the probability of the outcomes plotted against the residuals. There is no stray point in the line. The residuals and predicted responses are displayed in Figure 5 (b). The red line's upper limit contains all of the data. Thus, it can be said that the model is appropriate. Figure 5(c) depicts a comparison of the actual and projected values. The linear

line becomes the center of all points. Given these findings, it is reasonable to infer that the suggested mathematical model was suitable and efficient for the evaluation of MB adsorption by ALG-BGs membranes.
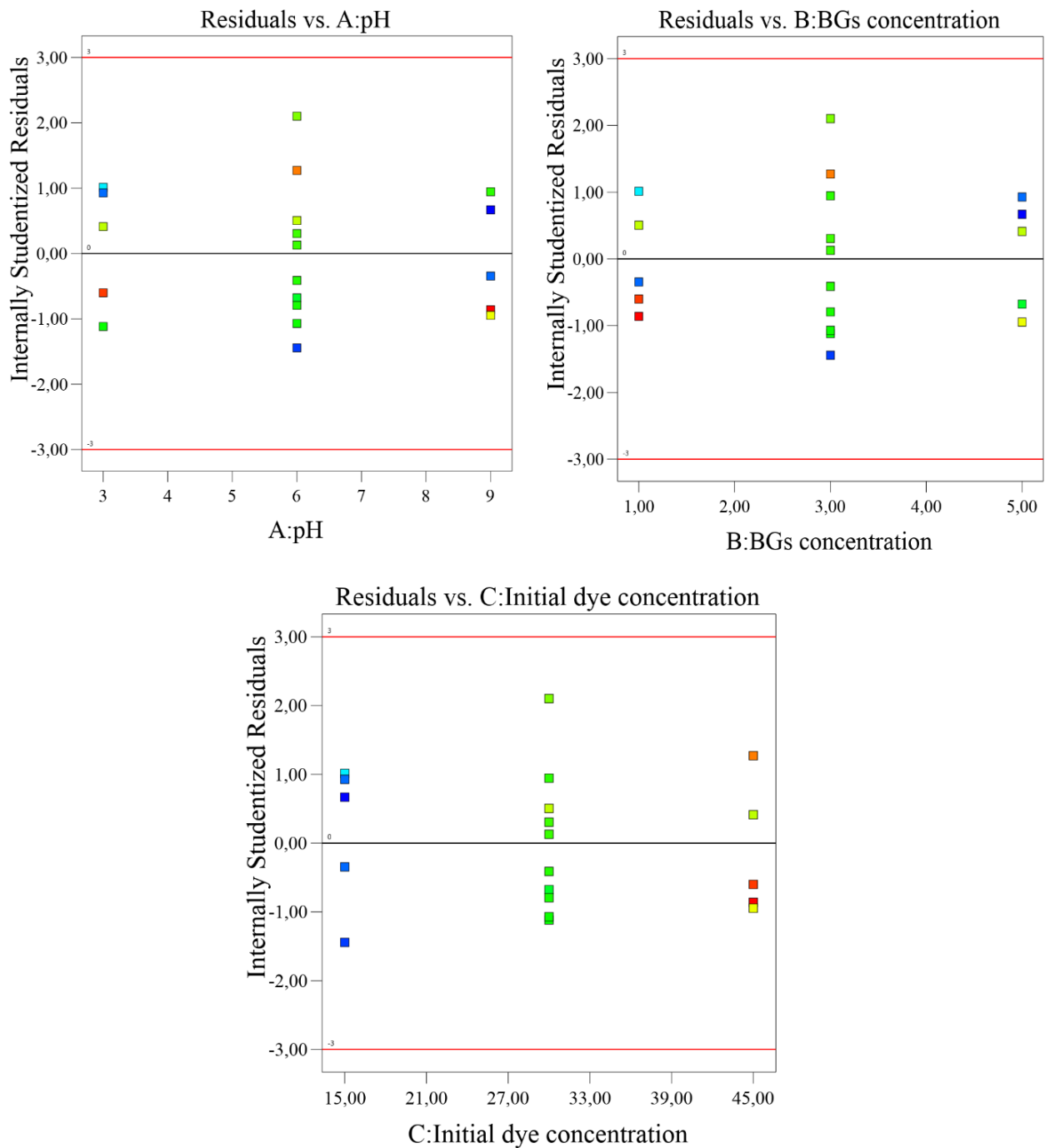


**Figure 4.** Diagnostic plots of residuals against factors

### 3.4. Isotherms studies

Adsorption tests using an ALG-1 membrane were carried out with starting MB levels ranging from 5 to 45 mg L$^{-1}$ in order to learn more about how the initial MB level impacts the effectiveness of the adsorption process. The pH and contact time in this experiment were kept constant at 9 and 120 min, respectively. To accurately describe the relationship between MB and ALG-1 adsorbents at equilibrium, various models, including the Langmuir, Freundlich, and Dubinin-Radushkevich (D-R) isotherms, were utilized to explain results. These models provide some understanding of how the accessible adsorption sites are distributed throughout the surface of adsorbent and aid in understanding mechanism of adsorption.

a)

Normal Plot of Residuals

b)

Residuals vs. Predicted

c)

Predicted vs. Actual
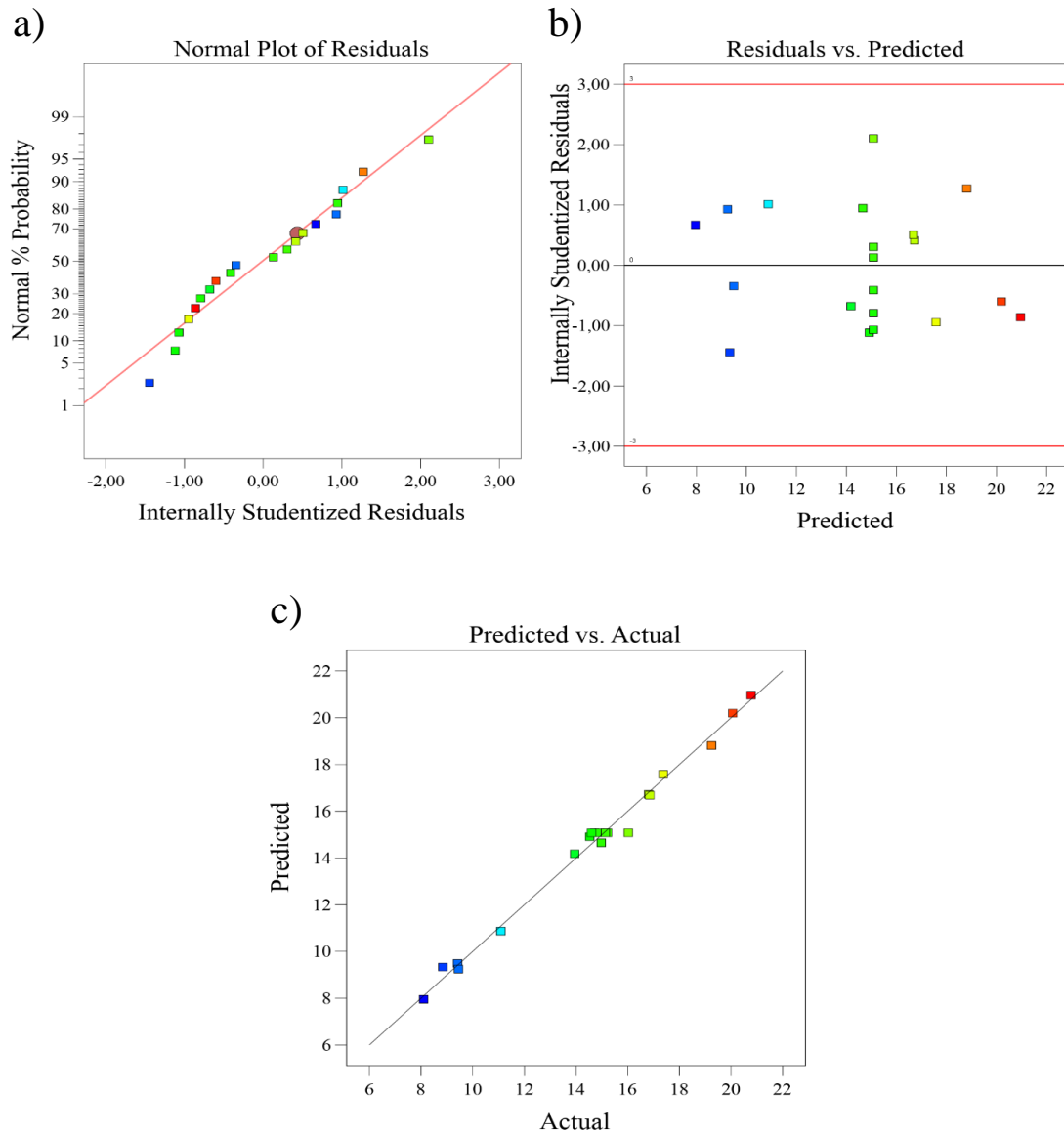
**Figure 5.** Diagnostic plots of normal probability against residuals (a), residuals against predicted responses (b), and predicted results against actual results (c)

Linear forms of Langmuir, Freundlich, and Dubinin-Radushkevich isotherms are defined by equations (4), (5), and (6), respectively (Allouss et al., 2019).

$$\frac{1}{q_e} = \frac{1}{q_m} + \frac{1}{bq_mC_e} \tag{4}$$

$$log\ q_e = log\ K_F + \left(\frac{1}{n}\right) log\ C_e \tag{5}$$

$$\ln(q_e) = \ln(q_m) - \beta\varepsilon^2 = RT\left(\ln\left(1 + \frac{1}{C_e}\right)\right) \tag{6}$$

where $q_e$ represents the equilibrium adsorption capacity (mg g$^{-1}$), $C_e$ indicates dye level at equilibrium (mg L$^{-1}$), $b$ shows Langmuir constant (L mg$^{-1}$), $q_m$ demonstrates maximum capacity for adsorption (mg g$^{-1}$), $K_F$ represents Freundlich constant, $n$ is heterogeneity factor and $\beta$ shows a constant linked to free energy (mol$^2$ kJ$^{-2}$), $R$ and $T$ indicates the gas constant (8.314 J/ mol/K), absolute temperature (K), respectively. Linear fitting of Langmuir and Freundlich models to equilibrium data is shown in Figures 6 (a) and (b), respectively. Experimental constants for Langmuir and Freundlich are demonstrated in Table 3. We can reasonably infer from the high correlation coefficient ($R^2$) that Freundlich model offered a more accurate description of the

isotherm data when ALG-1 was used as an adsorbent. This demonstrates that MB is adsorbed onto the ALG-BGs membrane using a multilayer process on a heterogeneous surface (Marzban et al., 2021). Freundlich isotherm was utilized to reveal adsorption of MB onto hydrogel beads made of carboxymethyl cellulose, alginate, and graphene oxide, according to Allouss et al. (2019). In addition, results showed that $K_F$ was 2.06 for linear approaches of the Freundlich adsorption isotherm that is in range of 1-20, which would be considered promising for adsorption. Similar to this, if the value of *n* is greater than 1, adsorption intensity indicated by *n* reveals the suitability of the model for adsorption purposes (Batool et al., 2018).

Experimental adsorption data have been fitted employing Dubinin-Radushkevich isotherm model to investigate whether adsorption is a chemical or physical process (Figure 6 (c)). Table 3 contains the D-R isotherm constants for this model's adsorption free energy and the maximum adsorption determined by eq (7) for each. The following equation was employed to calculate mean free energy of adsorption (E*a*) using value of D-R isotherm constant (β):

$$Ea = \frac{1}{\sqrt{2\beta}} \tag{7}$$

On the basis of the literature, chemisorption is the rate-limiting step when free energy ($E_a$) value is higher than 16 kJ mol$^{-1}$, while physisorption is appropriate when the value is less than 8 kJ mol$^{-1}$ (Tan et al., 2018; Allouss et al., 2019). Since the value of $E_a$ in this study was higher than 8 kJ mol$^{-1}$ (Table 3), it is possible that chemical binding is the cause of the MB adsorption on the ALG-1 membrane. This leads to the conclusion that chemical processes rather than physical processes underlie the majority of MB binding to the ALG-BGs.
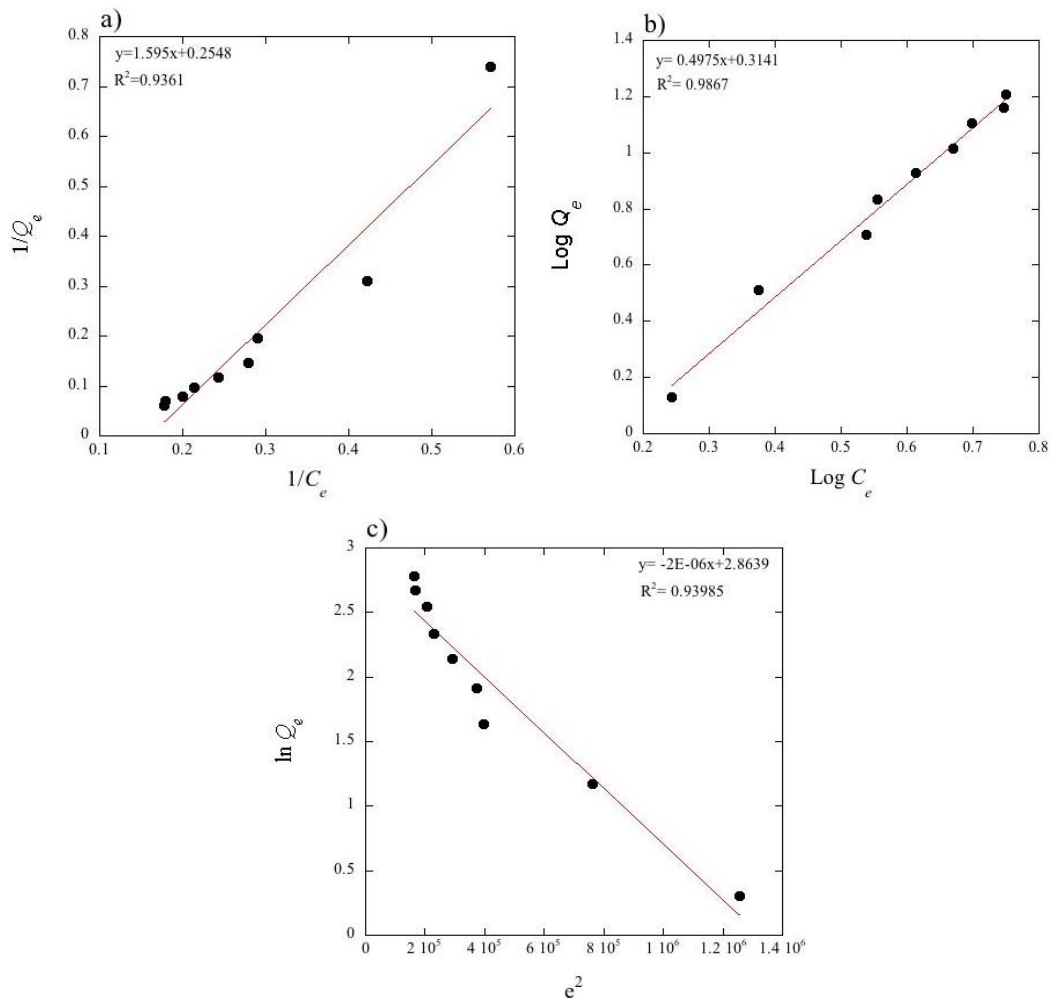


**Figure 6.** Linear fitting plots of the (a) Langmuir, (b) Freundlich, and (c) Dubinin–Radushkevich isotherms.

**Table 3.** Parameters of the isotherm for MB adsorption on the membranes of ALG-1

| Models | Parameters | Values |
|---|---|---|
| Langmuir | $q_m$ (mg g$^{-1}$) | 3.92 |
| | $b$ (L mg$^{-1}$) | 0.16 |
| | $R^2$ | 0.9361 |
| Freundlich | $K_F$ | 2.06 |
| | $n$ | 2.01 |
| | $R^2$ | 0.9867 |
| Dubinin-Radushkevich | $q_m$ (mg g$^{-1}$) | 17.53 |
| | $\beta$ ( mol$^2$ K$^{-2}$J$^{-2}$) | 2x10$^{-6}$ |
| | $E_a$ (KJ mol$^{-1}$) | 500 |
| | $R^2$ | 0.9399 |

## 3.5. Adsorption kinetics

The kinetics of adsorption were evaluated using an ALG-1 sample with an initial MB level of 45 mg $^{-1}$, pH of 9.0, and a contact time of 5 to 120 min. To understand adsorption kinetics of MB onto ALG-1 membrane, pseudo-1$^{st}$-order and pseudo-2$^{nd}$-order models were used to fit experimental results (Ma et al., 2019). Eq (8) represents equation of a pseudo-1$^{st}$-order kinetic model.

$$\ln(q_e - q_t) = lnq_e - k_1 t \tag{8}$$

where $q_e$ and $q_t$ indicate amounts of dye adsorbed on adsorbent (mg g$^{-1}$) at equilibrium and at time $t$, respectively, and $k_1$ is equilibrium rate constant of pseudo-1st-order model (min$^{-1}$), Table 4 shows levels of rate constant $k_1$, predicted $q_e$ , and $R^2$.

Linear equation for the pseudo-2$^{st}$ order kinetic model is depicted in equation below:

$$\frac{t}{q_t} = \frac{1}{k_2 q_e^2} + \frac{t}{q_e} \tag{9}$$

where $q_e$ and $q_t$ indicates adsorption capacities (mg g$^{-1}$) at equilibrium and time ($t$), respectively, and $k_2$ is pseudo-2$^{nd}$-order model's equilibrium rate constant (g mg$^{-1}$ min$^{-1}$). Table 4 lists values of rate constant $k_2$, predicted $q_e$, and $R^2$.

Adsorption kinetics parameters for pseudo-1$^{st}$-order and pseudo-2$^{nd}$-order models, respectively, were estimated using linear plots in Figures 7 (a) and (b), and findings are listed in Table 4. The information in Table 4 indicates that pseudo-second-order kinetic model's $R^2$ for a level of 45 mg L$^{-1}$ is significantly higher than pseudo-first-order kinetic model's $R^2$. The fact that theoretical $q_e$ values agree with the experimental data reveals that this adsorption process is governed by pseudo-second-order kinetics. The pseudo-second-order model, in which amount of accessible active sites in the ALG-BGs adsorbent greatly influences MB adsorption efficiency, is therefore a better fit for experimental kinetic data for MB adsorption (Allouss et al., 2019; Alver et al., 2020).

**Table 4.** Parameters for kinetic model of MB adsorption on the ALG-1 membrane

| Models | Parmeters | Values |
|---|---|---|
| Pseudo-first order kinetic | $q_{e,\ exp}$ (mg g$^{-1}$) | 2.86 |
| | $k_1$ (min$^{-1}$) | 0.00027 |
| | $q_{e,\ calc}$ (mg g$^{-1}$) | 15.5 |
| | $R^2$ | 0.8913 |
| Pseudo-second order kinetic | $q_{e,\ exp}$ (mg g$^{-1}$) | 15.5 |
| | $k_2$ (g mg$^{-1}$ min$^{-1}$) | 0.03116 |
| | $q_{e,\ calc}$ (mg g$^{-1}$) | 15.7 |
| | $R^2$ | 0.9997 |
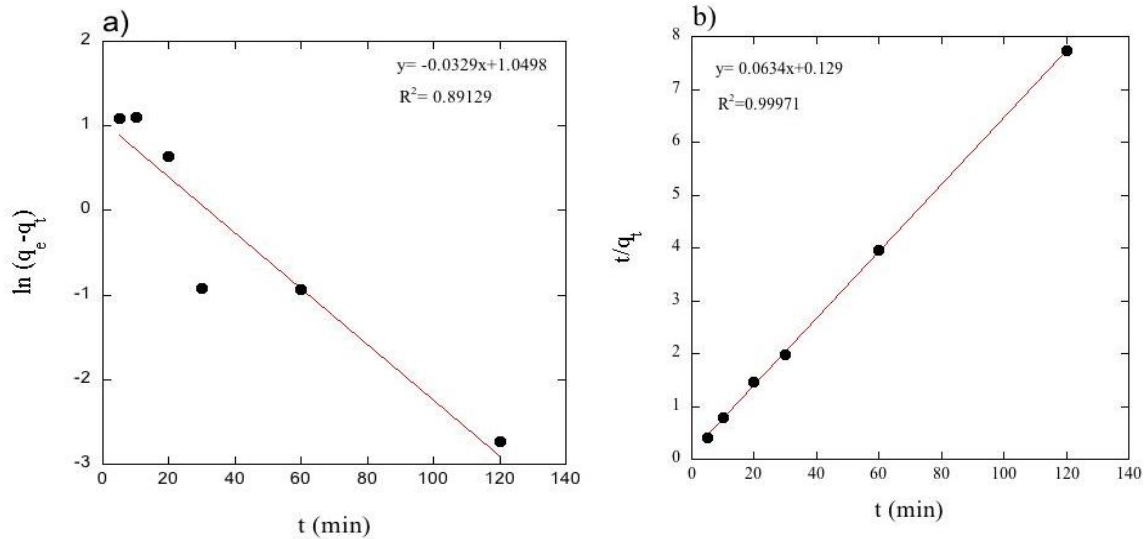
**Figure 7.** Kinetics of adsorption of MB dye on ALG-1 membrane: (a) Pseudo-first order-kinetic; (b) Pseudo second-order kinetic models

### 3.6. Proposed adsorption mechanism

The nature of an adsorbate, the characteristics of an adsorbent, and any potential interactions between an adsorbate and an adsorbent all affect how a pollutant is absorbed onto that material. A model of the MB adsorption mechanism was presented (Figure 8). The electrostatic forces and hydrogen bonds formed by the free Si-O- present in BGs, as well as some alginate OH groups that did not interfere with the crosslinking process, could be used to deduce the MB dye removal mechanism. As shown, the mechanism is connected to two different interactions. The electrostatic attraction force was attributed to the first interaction, which results from the difference in charges between the molecules of MB and surface material of the BG. Hydrogen bonding between dye's amine groups and the hydroxyl groups in adsorbent membranes was said to be responsible for the second one (Boukoussa et al., 2021; Mokhtar et al., 2020).
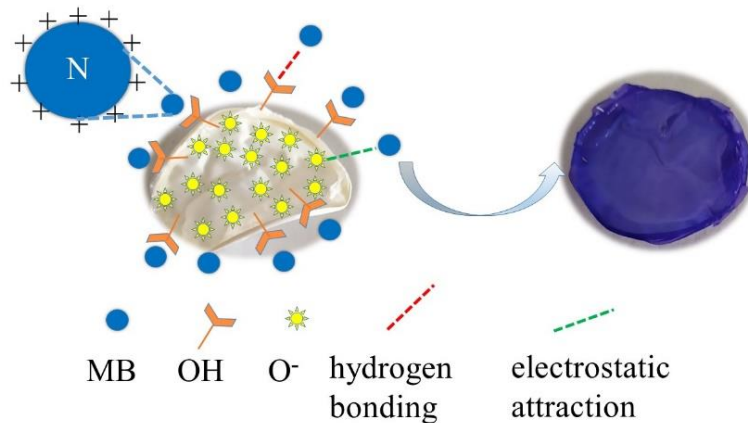


**Figure 8.** Proposed adsorption mechanism of MB on ALG-BGs membrane

### 4. Conclusions

In this work, BGs particles obtained by the modified Stöber method were incorporated into an alginate biopolymer to prepare composite membranes for the removal of MB dye. DLS analysis and TEM results showed that BGs particles exhibited good water dispersibility and were homogeneous in size and form. According to an AFM analysis, the roughness of the membranes increased with BGs concentration. An efficient and trustworthy strategy for maximizing adsorption parameters for MB removal was offered by the RSM-CCD model. Significant regression coefficients were achieved ($R^2$-value 99.09% and adjusted $R^2$-value 98.27%), which demonstrated that adsorption process is controlled by a polynomial quadratic model. At pH =

9, initial MB level of 45 mg L$^{-1}$, and BGs concentration of 1% w/v, the optimal values were found, at which point maximum removal rate was attained. The Freundlich model provided a good description of experimental data on adsorption. ($R^2$= 0.9867). Kinetics studies indicated that the MB adsorption process on ALG-1 membrane was dominated by a pseudo-second-order mechanism ($R^2$= 0.9997). Based on value of $E_a$ obtained from D–R model, the dominant mechanism of MB adsorption was chemical adsorption. Due to their biocompatibility and biosafety, the produced ALG-BGs membranes could therefore be used as candidates for the removal of dye pollutants.

**Author contribution**

Hasan Türe completed all stages of the study, including the preparation and characterization of samples, research, statistical analysis, etc.

**Declaration of ethical code**

For this investigation, no specific ethical approval was required.

**Conflicts of interest**

There are no apparent conflicts.

**References**

Abdullah, Z. W., Dong, Y., Han, N., & Liu, S. (2019). Water and gas barrier properties of polyvinyl alcohol (PVA)/starch (ST)/glycerol (GL)/halloysite nanotube (HNT) bionanocomposite films: Experimental characterisation and modelling approach. *Composites Part B: Engineering, 174*, 107033.https://doi.org/ 10.1016/j.compositesb.2019.107033

Allouss, D., Essamlali, Y., Amadine, O., Chakir, A., & Zahouily, M. (2019). Response surface methodology for optimization of methylene blue adsorption onto carboxymethyl cellulose-based hydrogel beads: adsorption kinetics, isotherm, thermodynamics and reusability studies. *RSC Advances*, *9*(65), 37858-37869. https://doi.org/10.1039/c9ra06450h

Al-Sakkari, E. G., Abdeldayem, O. M., Genina, E. E., Amin, L., Bahgat, N. T., Rene, E. R., & El-Sherbiny, I. M. (2020). New alginate-based interpenetrating polymer networks for water treatment: A response surface methodology based optimization study. *International Journal of Biological Macromolecules*, *155*, 772-785. https://doi.org/10.1016/j.ijbiomac.2020.03.220

Alver, E., Metin, A. Ü., & Brouers, F. (2020). Methylene blue adsorption on magnetic alginate/rice husk bio-composite. *International Journal of Biological Macromolecules*, *154*, 104-113. https://doi.org/10.1016/j.ijbiomac.2020.02.330

Baloch, H. A., Nizamuddin, S., Siddiqui, M. T. H., Riaz, S., Jatoi, A. S., Dumbre, D. K., Griffin, G. (2018). Recent advances in production and upgrading of bio-oil from biomass: A critical overview. *Journal of environmental chemical engineering*, *6*(4), 5101-5118. https://doi.org/10.1016/j.jece.2018.07.050

Batool, F., Akbar, J., Iqbal, S., Noreen, S., & Bukhari, S. N. A. (2018). Study of isothermal, kinetic, and thermodynamic parameters for adsorption of cadmium: an overview of linear and nonlinear approach and error analysis. *Bioinorganic Chemistry and Applications*, https://doi.org/10.1155/2018/3463724

Boukhalfa, N., Boutahala, M., Djebri, N., & Idris, A. (2019). Kinetics, thermodynamics, equilibrium isotherms, and reusability studies of cationic dye adsorption by magnetic alginate/oxidized multiwalled carbon nanotubes composites. *International Journal of Biological Macromolecules*, *123*, 539-548. https://doi.org/j.ijbiomac.2018.11.102

Boukoussa, B., Mokhtar, A., El Guerdaoui, A., Hachemaoui, M., Ouachtak, H., Abdelkrim, S., Bengueddach, A. (2021). Adsorption behavior of cationic dye on mesoporous silica SBA-15 carried by calcium alginate beads: Experimental and molecular dynamics study. *Journal of Molecular Liquids*, *333*, 115976. https://doi.org/10.1016/j.molliq.2021.115976

Djelad, A., Mokhtar, A., Khelifa, A., Bengueddach, A., & Sassi, M. (2019). Alginate-whey an effective and green adsorbent for crystal violet removal: Kinetic, thermodynamic and mechanism studies. *International Journal of Biological Macromolecules*, *139*, 944-954. https://doi.org/10.1016/j.ijbiomac.2019.08.068

Dlamini, D. S., Tesha, J. M., Vilakati, G. D., Mamba, B. B., Mishra, A. K., Thwala, J. M., & Li, J. (2020). A critical review of selected membrane-and powder-based adsorbents for water treatment: Sustainability and effectiveness. *Journal of Cleaner Production*, *277*, 123497. https://doi.org/j.jclepro.2020.123497

Dziadek, M., Menaszek, E., Zagrajczuk, B., Pawlik, J., & Cholewa-Kowalska, K. (2015). New generation poly (ε-caprolactone)/gel-derived bioactive glass composites for bone tissue engineering. *Materials Science and Engineering: C*, *56*, 9-21. https://doi.org/10.1016/j.msec.2015.06.020

Godiya, C. B., Liang, M., Sayed, S. M., Li, D., & Lu, X. (2019). Novel alginate/polyethyleneimine hydrogel adsorbent for cascaded removal and utilization of $Cu2^+$ and $Pb^{2+}$ ions. *Journal of Environmental Management*, *232*, 829-841. https://doi.org/10.1016/j.jenvman.2018.11.131

Karimifard, S., & Moghaddam, M. R. A. (2018). Application of response surface methodology in physicochemical removal of dyes from wastewater: a critical review. *Science of the Total Environment*, *640*, 772-797. https://doi.org/10.1016/j.scitotenv.2018.05.355

Katheresan, V., Kansedo, J., & Lau, S. Y. (2018). Efficiency of various recent wastewater dye removal methods: A review. *Journal of environmental chemical engineering*, *6*(4), 4676-4697. https://doi.org/10.1016/j.jece.2018.06.060

Li, L., Chen, L., Shi, H., Chen, X., & Lin, W. (2016). Evaluation of mesoporous bioactive glass (MBG) as adsorbent for removal of methylene blue (MB) from aqueous solution. *Journal of environmental chemical engineering*, *4*(2), 1451-1459. https://doi.org/10.1016/j.jece.2016.01.039

Ma, Y., Qi, P., Ju, J., Wang, Q., Hao, L., Wang, R., Tan, Y. (2019). Gelatin/alginate composite nanofiber membranes for effective and even adsorption of cationic dyes. *Composites Part B: Engineering*, *162*, 671-677. https://doi.org/10.1016/j.compositesb.2019.01.048.

Marzban, N., Moheb, A., Filonenko, S., Hosseini, S. H., Nouri, M. J., Libra, J. A., & Farru, G. (2021). Intelligent modeling and experimental study on methylene blue adsorption by sodium alginate-kaolin beads. *International Journal of Biological Macromolecules*, *186*, 79-91. https://doi.org/ 10.1016/j.ijbiomac.2021.07.006

Mensah, K., Mahmoud, H., Fujii, M., Samy, M., & Shokry, H. (2022). Dye removal using novel adsorbents synthesized from plastic waste and eggshell: mechanism, isotherms, kinetics, thermodynamics, regeneration, and water matrices. *Biomass Conversion and Biorefinery*, 1-16. https://doi.org/10.1007/s13399-022-03304-4

Mokhtar, A., Abdelkrim, S., Djelad, A., Sardi, A., Boukoussa, B., Sassi, M., & Bengueddach, A. (2020). Adsorption behavior of cationic and anionic dyes on magadiite-chitosan composite beads. *Carbohydrate Polymers*, *229*, 115399. https://doi.org/10.1016/j.carbpol.2019.115399

Mostafa, A. A., El-Sayed, M. M., Emam, A. N., Abd-Rabou, A. A., Dawood, R. M., & Oudadesse, H. (2021). Bioactive glass doped with noble metal nanoparticles for bone regeneration: in vitro kinetics and proliferative impact on human bone cell line. *RSC Advances*, 11(41), 25628-25638. https://doi.org/10.1039/d1ra03876a

Nidheesh, P., Zhou, M., & Oturan, M. A. (2018). An overview on the removal of synthetic dyes from water by electrochemical advanced oxidation processes. *Chemosphere*, *197*, 210-227. https://doi.org/ 10.1016/j.chemosphere.2017.12.195

Oladipo, A. A., Gazi, M., & Saber-Samandari, S. (2014). Adsorption of anthraquinone dye onto eco-friendly semi-IPN biocomposite hydrogel: equilibrium isotherms, kinetic studies and optimization. *Journal of the Taiwan Institute of Chemical Engineers*, *45*(2), 653-664. https://doi.org/10.1016/j.jtice.2013.07.013

Sabbagh, N., Tahvildari, K., & Sharif, A. A. M. (2021). Application of chitosan-alginate bio composite for adsorption of malathion from wastewater: Characterization and response surface methodology. *Journal of Contaminant Hydrology*, *242*, 103868. https://doi.org/10.1016/j.jconhyd.2021.103868

Suba, V., & Rathika, G. (2016). Novel adsorbents for the removal of dyes and metals from aqueous solution—a review. *Journal of Advanced Physics*, *5*(4), 277-294. https://doi.org/10.1166/jap.2016.1269

Tan, C. H. C., Sabar, S., & Hussin, M. H. (2018). Development of immobilized microcrystalline cellulose as an effective adsorbent for methylene blue dye removal. *South African journal of chemical engineering*, *26*, 11-24. https://doi.org/10.1016/j.sajce.2018.08.001

Tkaczyk, A., Mitrowska, K., & Posyniak, A. (2020). Synthetic organic dyes as contaminants of the aquatic environment and their implications for ecosystems: A review. *Science of the Total Environment*, *717*, 137222. https://doi.org/10.1016/j.scitotenv.2020.137222

Türe, H. (2019). Development of copper-doped bioglass/alginate composite membranes: Preliminary results on their characterization and antimicrobial properties. *Materials Today Communications*, *21*, 100583.https://doi.org/10.1016/j.mtcomm.2019.100583

Wang, B., Wan, Y., Zheng, Y., Lee, X., Liu, T., Yu, Z., Gao, B. (2019). Alginate-based composites for environmental applications: a critical review. *Critical Reviews in Environmental Science and Technology*, *49*(4), 318-356. https://doi.org/10.1080/10643389.2018.1547621

Zheng, K., Dai, X., Lu, M., Hüser, N., Taccardi, N., & Boccaccini, A. R. (2017). Synthesis of copper-containing bioactive glass nanoparticles using a modified Stöber method for biomedical applications. *Colloids and Surfaces B: Biointerfaces, 150*, 159-167. https://doi.org/10.1016/j.colsurfb.2016.11.016.

Zheng, K., Wu, J., Li, W., Dippold, D., Wan, Y., & Boccaccini, A. R. (2018). Incorporation of Cu-containing bioactive glass nanoparticles in gelatin-coated scaffolds enhances bioactivity and osteogenic activity. *ACS Biomaterials Science & Engineering, 4*(5), 1546-1557. https://doi.org/10.1021/acsbiomaterials.8b00051

Zhou, Y., Lu, J., Zhou, Y., & Liu, Y. (2019). Recent advances for dyes removal using novel adsorbents: a review. *Environmental Pollution*, *252*, 352-365. https://doi.org/10.1016/j.envpol.2019.05.072